


Cite this: *RSC Adv.*, 2017, 7, 25627

Effect of an improved gas diffusion cathode on carbamazepine removal using the electro-Fenton process

Wei Wang, Yaobin Lu, Haiping Luo, Guangli Liu * and Renduo Zhang

The aim of this study was to investigate the effect of the diffusion layer of a gas diffusion cathode (GDC) on H_2O_2 production to enhance carbamazepine removal using the electro-Fenton process. The diffusion layer was made by carbon black and polytetrafluoroethylene with sodium sulfate (Na_2SO_4) as a pore former. Different ratios of Na_2SO_4 to carbon black (w/w) (*i.e.*, 0%, 50%, 100%, 150%, and 200%) in the diffusion layer were tested. With an increase of the ratio, the average pore size in the diffusion layer and the electro-activity in the GDC increased simultaneously, which resulted in a higher mass transfer coefficient of oxygen and H_2O_2 production. In an undivided cell with platinum as the anode and $5.0 \text{ g L}^{-1} \text{ Na}_2\text{SO}_4$ as the electrolyte, a maximum H_2O_2 concentration of 630 mg L^{-1} was achieved within 120 min in the GDC with the ratio of 150%. With an initial carbamazepine concentration of 50 mg L^{-1} and a current density of 5.0 mA cm^{-2} , the maximum carbamazepine removal efficiency and rate reached 71% and $35.5 \text{ mg L}^{-1} \text{ h}^{-1}$, respectively. The removal rates in this study were much higher than those in the literature (35.5 vs. $0.03\text{--}10.0 \text{ mg L}^{-1} \text{ h}^{-1}$), mainly attributable to the diffusion layer modified by the pore former, which accelerated oxygen transfer and boosted H_2O_2 production. The results from this study should be useful to remove carbamazepine from wastewater treatment using the electro-Fenton (EF) process with improvement of pore structure in the diffusion layer of GDC.

Received 2nd April 2017

Accepted 5th May 2017

DOI: 10.1039/c7ra03793g

rsc.li/rsc-advances

1. Introduction

As effective methods for recalcitrant organic pollutant degradation in wastewater treatment, advanced oxidation processes, such as photocatalytic oxidation, Fenton, and ozonation,¹ have been applied. Highly reactive species such as hydroxyl radicals can be produced with strong oxidation capability to decompose many kinds of organic pollutants in the oxidation processes. The electro-Fenton (EF) process is a promising method to combine hydroxyl radicals produced in the Fenton reaction with electrochemistry.² Compared with the conventional Fenton process, the advantages of the EF process are as follows. On-site production of H_2O_2 can eliminate the potential risk of transportation and storage for H_2O_2 . The Fenton reaction can be automatically controlled and easily maintained. The Fe^{2+} catalyst can be regenerated at the anode ($\text{Fe}^{3+} + \text{e}^- \rightarrow \text{Fe}^{2+}$) and excess sludge can be minimized.^{3,4} Degradation of many refractory organic pollutants, such as phenol,⁵ 4-chlorophenol,⁶ and perfluorooctanoate,⁷ has been examined using the EF process. However, one of key limitations of EF applications is the low concentration of oxygen dissolved in the solution

according to the production reaction of hydrogen peroxide ($\text{O}_2 + 2\text{e}^- + 2\text{H}^+ \rightarrow \text{H}_2\text{O}_2$).^{4,8}

Usage of the gas diffusion cathode (GDC) is a promising way to accelerate oxygen diffusion and H_2O_2 production.^{4,8} The GDC is usually composed of three layers, that is, a diffusion layer, a current collector layer, and a catalyst layer.⁹ Because of high specific surface area and porosity of the diffusion layer, oxygen gas can efficiently pass through the diffusion layer and reach the interface between the catalyst layer and electrolyte, resulting in low energy consumption and high production of H_2O_2 . Therefore, the pore structure of the diffusion layer plays an important role in oxygen transfer, which has been studied for the fuel cells.^{4,9} Because of low costs, carbon black and polytetrafluoroethylene (PTFE) have been commonly used as the raw materials to make the diffusion layer.⁴ PTFE is used the binder of carbon black to form many pores as gas channels.⁸ Carbon- and PTFE-based GDC has been applied to remove refractory organics from solutions in the EF process.^{5,10}

As one of typical pharmaceuticals and personal care products, carbamazepine (CBZ) has been widely used.¹¹ The total consumption of CBZ is about 1014 t in the world each year, which accounted for 96% of the total pharmaceutical consumption in 2007.¹² However, overdose and metabolites of CBZ may result in damage of human's liver and emopoietic systems.¹³ CBZ has an amide structure that is stable and difficult to be degraded. The benzene ring of CBZ is a closed

Guangdong Provincial Key Laboratory of Environmental Pollution Control and Remediation Technology, School of Environmental Science and Engineering, Sun Yat-sen University, Guangzhou 510275, China. E-mail: liugl@mail.sysu.edu.cn



conjugate system and form π bond, resulting in high stability of CBZ.¹⁴ Moreover, the Henry coefficient of CBZ is as low as $1.09 \times 10^{-5} \text{ Pa m}^3 \text{ mol}^{-1}$ so that CBZ cannot be efficiently removed by the physical methods, such as air stripping treatment.^{15,16} The EF process has been utilized to degrade CBZ.^{17,18} Komtchou *et al.*¹⁷ demonstrated that 66% of 12 mg L^{-1} CBZ was removed within 120 min in the EF process under a current density of 1.8 mA cm^{-2} (0.2 A). A new material of carbon fiber coupled with cobalt phthalocyanine has been used as the cathode in the EF process, resulting in 97% of CBZ removal within 120 min.¹⁷ However, CBZ removal rates in the EF process are still low. For example, a CBZ removal rate of $4.0 \text{ mg L}^{-1} \text{ h}^{-1}$ with the EF process has been reported,¹⁷ which is only 40% of that in the Fenton-like process.¹⁹ To enhance the EF process, several strategies have been developed, including new catalysts, new configuration, *etc.*^{6,20,21} Nevertheless, the idea using the diffusion layer morphology to enhance the EF process on the recalcitrant organic pollutant removal has not been examined as far as we know.

The objective of this study was to investigate the effect of improved pore structure in the diffusion layer on H_2O_2 production to enhance CBZ degradation using the EF process. Different morphology and porosities of the diffusion layer with sodium sulfate (Na_2SO_4) as the pore former were characterized. Production of H_2O_2 and CBZ degradation in the EF process were determined. The mechanism of the effect of diffusion layer on the CBZ degradation was discussed.

2. Experiment

2.1 GDC preparation

The diffusion layer was prepared with Na_2SO_4 as the pore former as follows.^{8,22} Carbon black (EC-300J, Ketjenblack, Japan) of 1200 mg was mixed with each of different Na_2SO_4 dosages to obtain mass ratios of Na_2SO_4 to carbon black of 0%, 50%, 100%, 150%, and 200%. Each mixture was added with 30 mL of ethyl alcohol and stirred with ultrasonic treatment for 30 min. A PTFE emulsion (60 wt%, Hesen electric Co. Ltd., Shanghai, China) of 2800 mg was then added slowly into the mixture with agitation and ultrasonic treatment for 30 min. After excess alcohol evaporated at room temperature, the final mixture with dough-like was rolled on the stainless steel mesh (90 meshes, length \times width \times thickness = $8 \text{ cm} \times 4 \text{ cm} \times 0.2 \text{ mm}$) and formed 0.8 mm thickness of diffusion layer. The catalyst layer in the GDC was prepared as the same as the diffusion layer, except with a mass ratio 3 : 1 of carbon black to PTFE without Na_2SO_4 addition. The catalyst layer was formed by rolling on another side of the stainless steel mesh. The GDC was boiled in the deionized water for 10 min and repeated for three times to remove Na_2SO_4 in the diffusion layer. Finally, the GDC was dried at 105°C for 12 h. A GDC without Na_2SO_4 addition was sintered at 450°C for 30 min and taken as the control. The total thickness of GDC was about 1 mm.

2.2 Reactor setup and operation

Undivided reactor was constructed with a cube plexiglass ($4 \text{ cm} \times 4 \text{ cm} \times 4 \text{ cm}$). A hole in diameter of 3 cm was made in

the cube plexiglass with an effective volume of 28 mL (diameter \times length = $3 \text{ cm} \times 4 \text{ cm}$). The GDC had an effective area of 7 cm^2 with a diameter of 3.0 cm. The distance between the anode and cathode was 4 cm. The length and diameter of the Pt anode were 3.3 cm and 0.5 mm, respectively. A Na_2SO_4 solution of 5 g L^{-1} as the supporting electrolyte and a current density of 50.0 A m^{-2} were used throughout all the tests. A solution of 50 mg L^{-1} CBZ was used in the undivided reactor for the experiments.

2.3 Measurements and calculations

The diffusion layer morphology was observed using a Field Emission Scanning Electron Microscope (FESEM, JSM-6330F, Electron Corp., Japan). Porosities of the diffusion layer on the stainless steel meshes were determined using an automatic specific surface area and porosity analyzer (ASAP, 2020 (M), Micromeritics Corp., USA). Pore structures and distributions in the diffusion layers were determined using the N_2 sorption-desorption method.

Oxygen transfer in the diffusion layer was measured in a sealed glass bottle with 100 mL of 5 g L^{-1} Na_2SO_4 solution. The diffusion layer with an effective surface area of 7 cm^2 was installed at one side of the glass bottle as the separator between the Na_2SO_4 solution inside and the air outside. Before the tests, the Na_2SO_4 solution was aerated by pure N_2 at least 15 min to keep the dissolved oxygen concentration $< 1 \text{ mg L}^{-1}$. Then dissolved oxygen concentrations in the Na_2SO_4 solution were recorded with a dissolved oxygen meter (YSI 550A, Xylem Inc., USA). The mass transfer coefficient of oxygen was calculated as follows:^{23,24}

$$k_0 = -\frac{V}{At} \ln\left(\frac{C_1 - C_2}{C_1}\right) \quad (1)$$

where V is the liquid volume in the sealed gas bottle (100 mL), A is the projected surface area of the diffusion layer (7 cm^2), and C_1 and C_2 are the saturated oxygen concentration (mg L^{-1}) and dissolved oxygen concentration (mg L^{-1}) in the sealed gas bottle at time t , respectively. The linear sweep voltammetry (LSV) measurement was carried out using an electrochemical station (CHI 660C, Shanghai Chenhua Inc., China). The calomel electrode, Pt anode, and the GDC were used as the reference electrode, the counter electrode, and the working electrode, respectively. The scan range was from 0.0 to -2500 mV with a scan rate of 10 mV s^{-1} . Before the LSV measurements were carried out, the reactors including the GDCs were fulfilled with the electrolyte at least for 24 h to reach a stable balance among electrolyte, oxygen, and the GDCs.

The H_2O_2 concentration was determined by the colorimetric standard method.²⁵ The CBZ concentration was determined with a high pressure liquid chromatograph (HPLC, P230II, Dalian Yilite analytic Instrument Co. Ltd., China). The mobile phase was the acetonitrile solution (50%, v/v). The CBZ removal efficiency was estimated by

$$E = 100\% \frac{C_0 - C_1}{C_0} \quad (2)$$



where E is the CBZ removal efficiency (%), and C_0 and C_1 are the initial and final CBZ concentrations (mg L^{-1}), respectively. The CBZ removal rate was calculated by

$$R = \frac{C_0 - C_1}{t} \quad (3)$$

where R is the CBZ removal rate ($\text{mg L}^{-1} \text{ h}^{-1}$) and t is the reaction time (h).

3. Results and discussions

3.1 Characterization of gas diffusion layer in the cathode

The SEM images on the surface morphology of diffusion layers using different Na_2SO_4 dosages as pore former are shown in Fig. 1. With increase of the ratios of Na_2SO_4 to carbon black from 0% to 200%, the surface morphology in the diffusion layers became coarser and more porous. As shown in Fig. 2, the ranges of pore sizes from 4 to 80 nm were similar among the different diffusion layers. However, the proportions of larger pores (>20 nm) were greater in the diffusion layers with higher amount of Na_2SO_4 . The characteristics of the diffusion layers with the different ratios of Na_2SO_4 to carbon black are listed in Table 1. Average pore sizes in the diffusion layers with the different ratios of Na_2SO_4 to carbon black were in the order of 19.3 nm (200%) $>$ 18.7 nm (150%) $>$ 18.1 nm (100%) $>$ 17.5 nm (50%) $>$ 17.1 nm (CK) $>$ 16.6 nm (0%). Total porosities in the different diffusion layers changed from 10.1% to 29.1% with

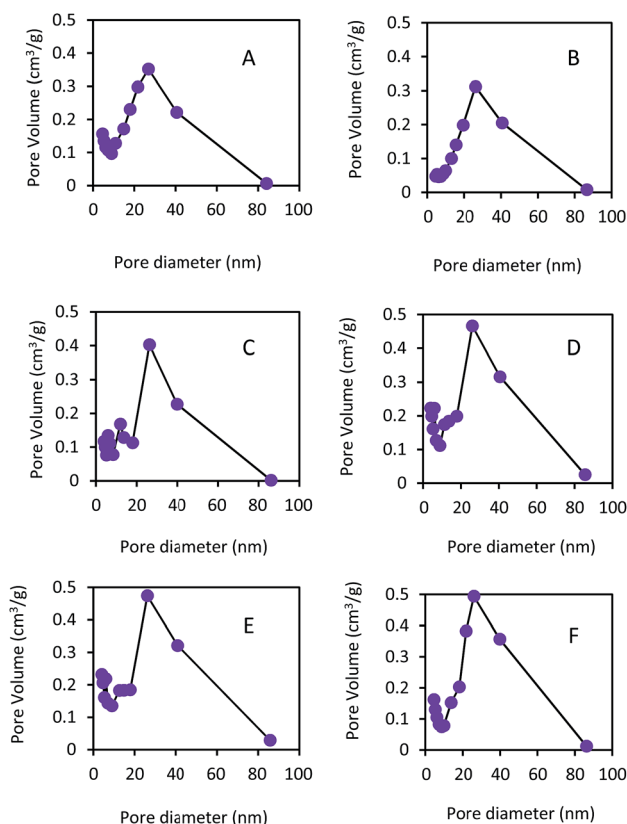


Fig. 2 The pore size distributions of the diffusion layer with different content of pore former for (A) the control, and with ratios of Na_2SO_4 to carbon black of (B) 0%, (C) 50%, (D) 100%, (E) 150%, and (F) 200%.

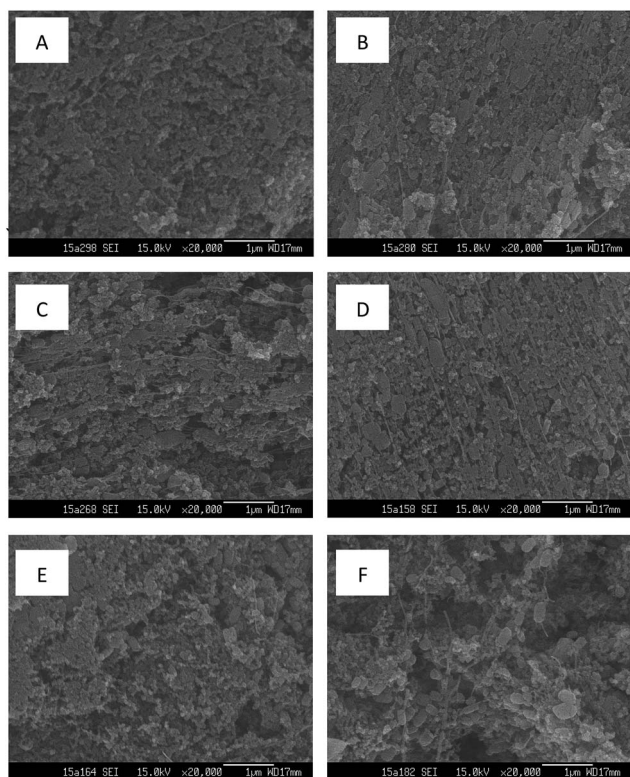


Fig. 1 SEM images on morphology of the diffusion layer for (A) the control check, and with ratios of Na_2SO_4 to carbon black of (B) 0%, (C) 50%, (D) 100%, (E) 150%, and (F) 200%.

increase of the ratios. The result of increase of pore sizes and porosities in the diffusion layers with the Na_2SO_4 amount was consistent with those reported in the polymer electrolyte fuel cells (PEFCs).^{26,27} Pores in the diffusion layers of the fuel cell could be increased by adding 20% (wt%) ammonium salt as pore former.²⁶ With increase of sucrose dosages from 25 to 75 (w/o) as pore former in the diffusion layer of the fuel cell, the porosity of diffusion layer increased from 36% to 50%.²⁷

The k_0 values increased with the ratios of Na_2SO_4 to carbon black, that is, $19.1 \times 10^{-4} \text{ cm s}^{-1}$ (200%) $>$ $18.0 \times 10^{-4} \text{ cm s}^{-1}$ (150%) $>$ $17.2 \times 10^{-4} \text{ cm s}^{-1}$ (100%) $>$ $17.0 \times 10^{-4} \text{ cm s}^{-1}$ (50%) $>$ $15.8 \times 10^{-4} \text{ cm s}^{-1}$ (CK) $>$ $15.2 \times 10^{-4} \text{ cm s}^{-1}$ (0%). The k_0 values were linearly correlated to the porosities (with a correlation coefficient $R = 0.973$), indicating that the mass transfer capacity of oxygen was attributable to the porosity in the diffusion layers. However, a severely water leakage in the diffusion layer occurred when the ratio of Na_2SO_4 to carbon black increased to 300% (data not shown). To keep a stable H_2O_2 production, the maximum ratio of Na_2SO_4 to carbon black was kept at 200% (w/w) in the following tests. The k_0 values in the diffusion layer was much higher than those in cation exchange membrane ($0.94 \times 10^{-4} \text{ cm s}^{-1}$) and ultrafiltration membrane ($0.19 \times 10^{-4} \text{ cm s}^{-1}$),²³ suggesting that the diffusion layer made by carbon black had higher oxygen transfer capacity than those by other materials. The k_0 values in this study were

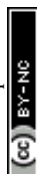


Table 1 Characteristics of the diffusion layers with different ratios of Na₂SO₄ to carbon black

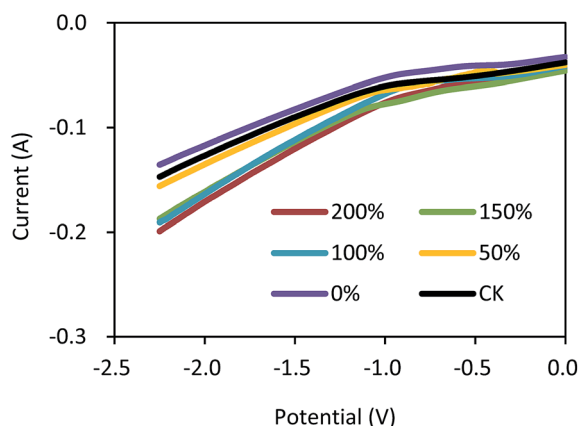
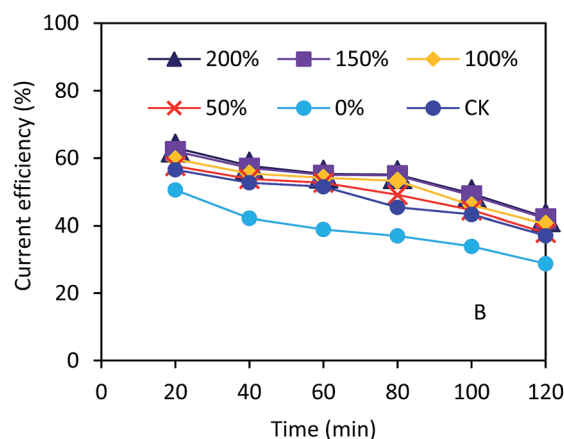
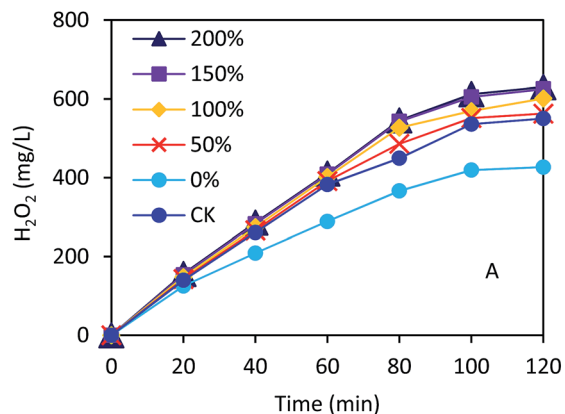
Ratio of Na ₂ SO ₄ to carbon black	Total porosity (%)	Average pore size (nm)
0%	10.1	16.6
50%	20.2	17.5
100%	24.1	18.1
150%	27.3	18.7
200%	29.1	19.3
Control check	15.3	17.1

comparable to the mass transfer coefficient ($27.0 \times 10^{-4} \text{ cm s}^{-1}$) in the electrochemical generation of H₂O₂.³ Moreover, the heat treatment (300–500 °C) of carbon black could increase carbon–oxygen surface groups on the carbon black particles and improve the lap shear strength of the adhesive joint between carbon black and adhesive.²⁸

3.2 Performance of gas diffusion cathode

The linear sweep voltammetry measurements in different GDCs are shown in Fig. 3. With the different ratios of Na₂SO₄ to carbon black (w/w) in the diffusion layer, GDCs showed different oxidation and reduction activities with the same catalyst layers. At the potential of −2.0 V, the maximum current reached −0.171 A using the GDC with the ratio of 200%. GDCs with the ratios of 150% and 100% had almost the same current of −0.162 A. The maximum current of −0.117 A was obtained in the GDC with the ratio of 0%. The result demonstrated that Na₂SO₄ as pore former could enhance the activity of GDC, which was consistent with those with other pore-forming agents, such as (NH₄)₂C₂O₄, NH₄HCO₃, NaCl, and PEG-200, reported in the literature.²⁹ Large average pore sizes and high mass transfer coefficients in the diffusion layers could result in high oxidation–reduction activity of GDCs according to the diffusion layer characteristics mentioned above.

As shown in Fig. 4A, the H₂O₂ concentrations increased with the operation time under the current density of 5.0 mA cm^{−2}.

**Fig. 3** Linear sweep voltammetry measurement on the gas diffusion cathode with different ratios of Na₂SO₄ to carbon black.**Fig. 4** (A) H₂O₂ concentration and (B) current efficiency in the electrochemical cell using the gas diffusion cathode with different ratios of Na₂SO₄ to carbon black.

The GDCs with the ratios of 150% and 200% had almost the same H₂O₂ concentration of 630 mg L^{−1} within 120 min. The H₂O₂ concentrations were 427, 562, and 601 mg L^{−1} with the ratios of 0%, 50%, and 100% within 120 min, respectively. The CK had higher H₂O₂ concentration than that with 0% Na₂SO₄ within 120 min (550 vs. 427 mg L^{−1}). The current efficiencies increased from 29% to 38% with the ratios from 0% to 50% within 120 min (Fig. 4B). However, the current efficiencies were not significantly improved and kept in a range of 38%–42% with the ratios from 50% to 200% within 120 min. The H₂O₂ concentrations and current efficiency in this study were comparable to those in other H₂O₂ electrochemical generation processes using GDCs.^{30,31} Nevertheless, our results demonstrated that the pore former could improve the H₂O₂ production in the electrochemical process, which should be important for the EF application in practice.

3.3 CBZ degradation in the electro-Fenton with different GDCs

Under the condition of current density of 5.0 mA cm^{−2} and 4.56 g L^{−1} ferrous sulfate, the CBZ removal efficiencies increased with the running time in the EF process (Fig. 5A). The



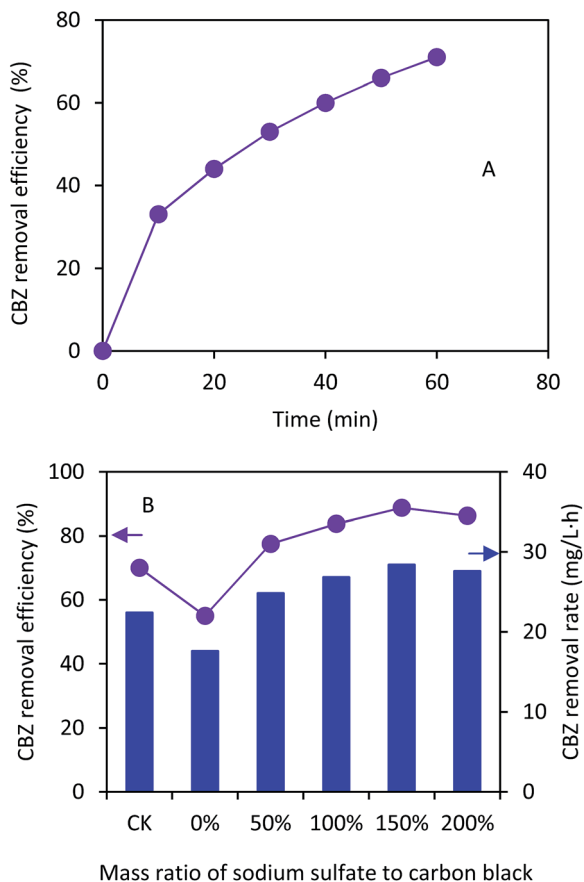


Fig. 5 (A) CBZ removal change with time in the electrochemical cell using the gas diffusion cathode with the Na_2SO_4 to carbon black ratio of 150% (w/w); (B) change with ratios of Na_2SO_4 to carbon black within 60 min (initial conditions: $4.56 \text{ g L}^{-1} \text{ FeSO}_4$, $50 \text{ mg L}^{-1} \text{ CBZ}$; operation conditions: $\text{pH} = 3.0$ and 5.0 mA cm^{-2} current density).

maximum CBZ removal efficiency reached 71% using the GDC with the ratio of Na_2SO_4 to carbon black of 150% within 60 min, which was much higher than that with 0% (44%) (Fig. 5B). The CBZ removal efficiencies were 62%, 67%, and 69% with the ratios of 50%, 100%, and 200%, respectively. The CBZ removal of the control (56%) was lower than that with the Na_2SO_4 addition, indicating that the pore former could enhance the EF process. The ratio of 200% resulted in lower CBZ removal than 150%, probably because of excess oxygen competition with CBZ during the EF process.³² Our results demonstrated that high concentration of CBZ (*e.g.* 50 mg L^{-1}) could be efficiently removed in the EF process. A control test showed that the adsorption of CBZ on the GDC was $9.8 \pm 0.5\%$ within 60 min. Therefore, the CBZ removal in the EF process was mainly attributed to the oxidation by hydroxyl radicals.

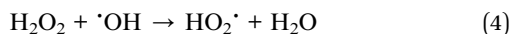
Table 2 compares the CBZ removal results based on the Fenton, electro-Fenton and Fenton-like processes. While the CBZ removal efficiencies with the different processes were comparable, the CBZ removal rates in this study were much higher than those in the literature.^{17–19,33,34} The highest CBZ removal rate reached $35.5 \text{ mg L}^{-1} \text{ h}^{-1}$ using the GDC, which was about five and nine times higher than those using the Fenton-like process with the initial CBZ concentration of 15 mg L^{-1} and $100 \text{ mM H}_2\text{O}_2$ ($7.5 \text{ mg L}^{-1} \text{ h}^{-1}$)³⁴ and the electro-Fenton process ($4.0 \text{ mg L}^{-1} \text{ h}^{-1}$),¹⁷ respectively. Full dosage of H_2O_2 was added at the beginning of the Fenton or Fenton-like process.^{19,33,34} The CBZ removal could take several hours *via* the Fenton or Fenton-like process, indicating that H_2O_2 was consumed gradually. However, residual H_2O_2 could compete with CBZ for exhausting the hydroxyl radical (eqn (4))³⁵ and hinder high CBZ removal rate:

Table 2 The comparison on the CBZ removal using different Fenton process

Methods	Initial concentration of CBZ (mg L^{-1})	Cathode catalyst	Current density (mA cm^{-2})	Reaction time (min)	Removal (%)	Removal rate ($\text{mg L}^{-1} \text{ h}^{-1}$)	Ref.
Fenton process	0.1	—	—	180	84	0.03	33
Fenton-like process	15	—	—	120	~100	~7.5	34
Fenton-like process	10	—	—	60	100	10.0	19
Electro-Fenton	12	Carbon felt cathode	1.8	120	66	4.0	17
	12		4.4	120	62	3.7	
	12		8.9	120	57	3.4	
	12		17.7	120	53	3.2	
Electro-Fenton	5.9	CoPc-CF ^a Carbon black with diffusion layer	—	120	97	2.9	18 This study
Electro-Fenton (0% Na_2SO_4)	50		5.0	60	44	22.0	
Electro-Fenton (50% Na_2SO_4)	50		5.0	60	62	31.0	
Electro-Fenton (100% Na_2SO_4)	50		5.0	60	67	33.5	
Electro-Fenton (150% Na_2SO_4)	50		5.0	60	71	35.5	
Electro-Fenton (200% Na_2SO_4)	50		5.0	60	69	34.5	

^a CoPc-CF: carbon fiber coupled with cobalt phthalocyanine.





In the electro-Fenton process with carbon felt or carbon fiber coupled with cobalt phthalocyanine (CoPc-CF) as cathode,^{17,18} without a diffusion layer in the cathode, the H_2O_2 concentration in the solution is usually pretty low. For example, the maximum H_2O_2 concentration was 1.44 mg L^{-1} after 120 min operation at the current density of 17.7 mA cm^{-2} (2.0 V) in the electro-Fenton with carbon felt cathode.¹⁷ Only 3.54 mg L^{-1} of the H_2O_2 concentration was produced after 30 min operation in the electro-Fenton with CoPc-CF cathode with an applied voltage of 2.5 V.¹⁸ However, because of high oxygen transfer coefficient in the diffusion layer of GDC, the H_2O_2 concentrations reached 150 mg L^{-1} within 20 min and 630 mg L^{-1} within 120 min operation in this study. The H_2O_2 concentrations gradually increased with the operation time, which reduced the chance of excess H_2O_2 accumulation and thus the reaction of eqn (4) might not occur. Therefore, high CBZ removal rate could be achieved in our electro-Fenton with GDC. Nevertheless, the CBZ removal varies with different conditions, including initial CBZ concentration, type of catalysts, current density, electrolytes, and others.^{17–19,33,34} It was difficult to make accurate comparison under the different conditions.

The GDC in the EF process is different from that in fuel cells, such as the proton exchange membrane fuel cell.^{26,29} Since the catalyst layer in the GDC in the EF process faces to aqueous solution, the diffusion layer in the EF should prevent the electrolyte leakage through the cathode.^{36,37} The specific requirement in the diffusion layer may limit the design of the pore structure of the diffusion layer using pore former, which should be further explored. Moreover, the life-time of the diffusion layer with pore former still needs to be investigated.

4. Conclusions

Different ratios of Na_2SO_4 to carbon black in the diffusion layer were investigated in the EF process for H_2O_2 production and CBZ removal. With increase of the ratios, the average pore size in the diffusion layer and the oxidation and reduction activity in the GDC increased simultaneously, resulting in high mass transfer coefficient of oxygen and H_2O_2 production. Under the current density of 5.0 mA cm^{-2} , the maximum H_2O_2 concentration of 630 mg L^{-1} was achieved with the ratio of 150% within 120 min. With the initial CBZ concentration of 50 mg L^{-1} and 5.0 mA cm^{-2} , the maximum CBZ removal efficiency and rate reached 71% and $35.5 \text{ mg L}^{-1} \text{ h}^{-1}$, respectively, using the GDC with the ratio of 150% within 60 min. Our experimental results demonstrated that the pore former can be used to optimize the pore structure of diffusion layer and to enhance the EF performance to CBZ removal in wastewater treatment.

Acknowledgements

This work was partly supported by grants from the National Natural Science Foundation of China (No. 51278500, 41471181, and 51308557), the Natural Science Foundation of Guangdong

Province (S2013010012984), the Science and Technology Program of Guangzhou (No. 201604010043), and the Fundamental Research Funds for the Central Universities (16lgjc65).

References

- 1 M. A. Oturan and J.-J. Aaron, *Crit. Rev. Environ. Sci. Technol.*, 2014, **44**, 2577–2641.
- 2 G. Ren, M. Zhou, M. Liu, L. Ma and H. Yang, *Chem. Eng. J.*, 2016, **298**, 55–67.
- 3 Z. Qiang, J.-H. Chang and C.-P. Huang, *Water Res.*, 2002, **36**, 85–94.
- 4 E. Brillas, I. Sirés and M. A. Oturan, *Chem. Rev.*, 2009, **109**, 6570–6631.
- 5 H. Luo, C. Li, C. Wu, W. Zheng and X. Dong, *Electrochim. Acta*, 2015, **186**, 486–493.
- 6 G. Santana-Martínez, G. Roa-Morales, E. Martín del Campo, R. Romero, B. A. Frontana-Urbe and R. Natividad, *Electrochim. Acta*, 2016, **195**, 246–256.
- 7 Y. Liu, S. Chen, X. Quan, H. Yu, H. Zhao and Y. Zhang, *Environ. Sci. Technol.*, 2015, **49**, 13528–13533.
- 8 H. Luo, C. Li, C. Wu and X. Dong, *RSC Adv.*, 2015, **5**, 65227–65235.
- 9 G. Inoue, K. Yokoyama, J. Ooyama, T. Terao, T. Tokunaga, N. Kubo and M. Kawase, *J. Power Sources*, 2016, **327**, 610–621.
- 10 E. Brillas, J. C. Calpe and J. Casado, *Water Res.*, 2000, **34**, 2253–2262.
- 11 P. Braeutigam, M. Franke, R. J. Schneider, A. Lehmann, A. Stolle and B. Ondruschka, *Water Res.*, 2012, **46**, 2469–2477.
- 12 D. P. Mohapatra, S. K. Brar, R. D. Tyagi, P. Picard and R. Y. Surampalli, *Talanta*, 2012, **99**, 247–255.
- 13 Y. Liu, S. Mei, D. Iya-Sou, S. Cavadias and S. Ognier, *Chem. Eng. Process.*, 2012, **56**, 10–18.
- 14 M. Suhasini, E. Sailatha, S. Gunasekaran and G. R. Ramkumar, *Spectrochim. Acta, Part A*, 2015, **141**, 252–262.
- 15 J. Sipma, B. Osuna, N. Collado, H. Monclús, G. Ferrero, J. Comas and I. Rodríguez-Roda, *Desalination*, 2010, **250**, 653–659.
- 16 Y. Zhang, S.-U. Geißen and C. Gal, *Chemosphere*, 2008, **73**, 1151–1161.
- 17 S. Komtchou, A. Dirany, P. Drogui and A. Bermond, *Environ. Sci. Pollut. Res.*, 2015, **22**, 11513–11525.
- 18 M. Liu, H. Xia, W. Lu, T. Xu, Z. Zhu and W. Chen, *J. Appl. Electrochem.*, 2016, 1–10.
- 19 V. M. Monsalvo, J. Lopez, M. Munoz, Z. M. D. Pedro, J. A. Casas, A. F. Mohedano and J. J. Rodriguez, *Chem. Eng. J.*, 2015, **264**, 856–862.
- 20 N. Li, J. An, L. Zhou, T. Li, J. Li, C. Feng and X. Wang, *J. Power Sources*, 2016, **306**, 495–502.
- 21 J. F. Pérez, J. Llanos, C. Sáez, C. López, P. Cañizares and M. A. Rodrigo, *Electrochem. Commun.*, 2016, **71**, 65–68.
- 22 H. Tang, S. Wang, M. Pan and R. Yuan, *J. Power Sources*, 2007, **166**, 41–46.
- 23 J. R. Kim, S. Cheng, S.-E. Oh and B. E. Logan, *Environ. Sci. Technol.*, 2007, **41**, 1004–1009.



- 24 X. Y. Zhang, S. A. Cheng, X. Wang, X. Huang and B. E. Logan, *Environ. Sci. Technol.*, 2009, **43**, 8456–8461.
- 25 *Standard Methods for the Examination of Water and Wastewater*, ed. L. S. Clesceri, A. E. Greenberg and A. D. Eaton, American Public Health Association, Washington, DC, 20th edn, 1998.
- 26 J. H. Chun, K. T. Park, D. H. Jo, J. Y. Lee, S. G. Kim, E. S. Lee, J.-Y. Jyoung and S. H. Kim, *Int. J. Hydrogen Energy*, 2010, **35**, 11148–11153.
- 27 G. Selvarani, A. K. Sahu, P. Sridhar, S. Pitchumani and A. K. Shukla, *J. Appl. Electrochem.*, 2008, **38**, 357–362.
- 28 S. W. Park and D. G. Lee, *Composites, Part A*, 2010, **41**, 1597–1604.
- 29 J. Liu, C. Yang, C. Liu, F. Wang and Y. Song, *Ind. Eng. Chem. Res.*, 2014, **53**, 5866–5872.
- 30 X. Yu, M. Zhou, G. Ren and L. Ma, *Chem. Eng. J.*, 2015, **263**, 92–100.
- 31 R. M. Reis, A. A. G. F. Beati, R. S. Rocha, M. H. M. T. Assumpção, M. C. Santos, R. Bertazzoli and M. R. V. Lanza, *Ind. Eng. Chem. Res.*, 2012, **51**, 649–654.
- 32 L. Zhou, M. Zhou, C. Zhang, Y. Jiang, Z. Bi and J. Yang, *Chem. Eng. J.*, 2013, **233**, 185–192.
- 33 D. P. Mohapatra, S. K. Brar, R. D. Tyagi, P. Picard and R. Y. Surampalli, *Sci. Total Environ.*, 2013, **447**, 280–285.
- 34 S. P. Sun, Z. Xia, C. Li and A. T. Lemley, *Chem. Eng. J.*, 2014, **244**, 44–49.
- 35 H. Zhang, D. Zhang and J. Zhou, *J. Hazard. Mater.*, 2006, **135**, 106–111.
- 36 T. Harrington and D. Pletcher, *J. Electrochem. Soc.*, 1999, **146**, 2983–2989.
- 37 Y. Lei, H. Liu, Z. Shen and W. Wang, *J. Hazard. Mater.*, 2013, **261**, 570–576.

